IMEKO TC6 International Conference on Metrology and Digital Transformation
September 19 – September 21, 2022, Berlin, Germany

UNCERTAINTY-AWARE ROOM-TEMPERATURE PROFILE ESTIMATION USING ORDINARY KRIGING

Anupam Prasad Vedurmudi [a,*], *Katharina Janzen* [a], *Sascha Eichstädt* [a]

[a]Physikalisch-Technische Bundesanstalt, Braunschweig/Berlin, Germany
[*]Corresponding author. E-mail address: anupam.vedurmudi@ptb.de

Abstract – Information leveraged from multiple sensors is generally more versatile than that from a single sensor. For instance, the value of a physical quantity at an unsampled location can be estimated by interpolating measurements from spatially separated sensors. In this contribution, kriging is used to spatially interpolate room temperatures from a limited number of sensors with different measurement uncertainties and a propagation of the sensor uncertainties to the interpolated values using a Monte Carlo simulation is demonstrated. A potential application of kriging to assess the quality of sensor measurements is also presented.

Keywords: Temperature, Sensor Fusion, Kriging, Uncertainty, Monte Carlo

1. INTRODUCTION

The widespread use of sensors and sensor networks is a key feature of the fourth industrial revolution or Industry 4.0 [1]. In order to fully exploit the large amount of information thus generated, sensor fusion methods [2] must be employed to combine measurement results from disparate sensors. By consolidating multi-sensor information in this way, insights, otherwise unavailable to individual sensors, become available. A key application of multi-sensor information is the interpolation of sensor data to estimate the value of a physical property at unsampled locations given a finite number of sensors placed at discrete locations [4]. In this contribution a method for estimating the room temperature using kriging is presented along with a Monte Carlo based method to estimate the associated measurement uncertainty. The sensor readings correspond to climate-controlled measurement rooms for large coordinate measuring machines that must conform to strict temperature requirements (see, for instance, [3]) in order to ensure the accuracy of their measurement results. In particular, a thought experiment involving the use of sensors with varying uncertainty characteristics will play a central role.

2. USE CASE

The system under study is that of a large temperature controlled room with an open cuboidal subvolume of dimensions 6.6 m×4.8 m×1.85 m used to perform high precision coordinate measurements on large objects. The temperature in the aforementioned region is measured by eight Pt100 platinum resistance thermometers such that seven are placed at its corners, while the remaining sensor is located at a height 0.25 m above the remaining corner due to the presence of measurement equipment unrelated to the present demonstration. The distribution of sensors in the measurement region under consideration is illustrated in Fig. 1. Measurements are taken from each sensor every five

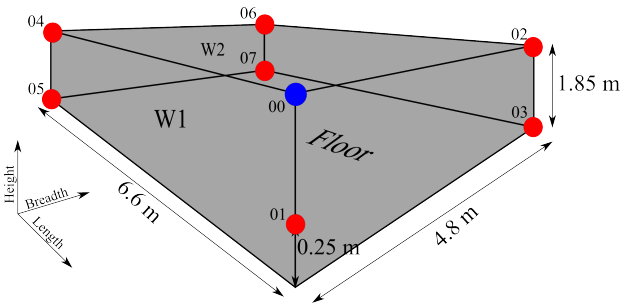

Fig. 1: The distribution of sensors in the subvolume of the room under consideration. Two of the boundaries (W1 & W2) and floor are indicated for future reference. The sensor indicated in blue (00) is assumed to have a lower uncertainty (25 mK) than the other sensors (100 mK) for the sake of the thought experiment.

minutes over a period of five days, i. e. 1440 readings per sensor. The measurements were taken at an interval of five minutes between 2nd December 2021 at 00:00 and 6th December 2021 at 23:55. The raw temperature measurements along with the respective hourly and daily rolling averages are shown in Fig. 2. The readings are distributed around 20 °C for the whole duration and sensor 07 shows a slight drop in temperature at around 17:45 on the last day.

2.1. *Measurement uncertainty*

The sensors used in the actual measurement setup are identical in terms of their calibration. For the purpose of the present demonstration, however, we assume that all but one of the sensors have a standard uncertainty of 100 mK, while the remaining one has an uncertainty of 25 mK. The sensor with the lower uncertainty (00) is indicated in blue in Fig. 1. Given the uncertainties and readings from the eight sensors, our goal is to estimate the temperature and associated measurement uncertainty at any point in the volume under consideration. In this regard we distinguish between the temperature interpolation, which is carried out on real data, and the uncertainty propagation, which corresponds to a thought experiment that demonstrates the use of sensors with heterogeneous uncertainty characteristics.

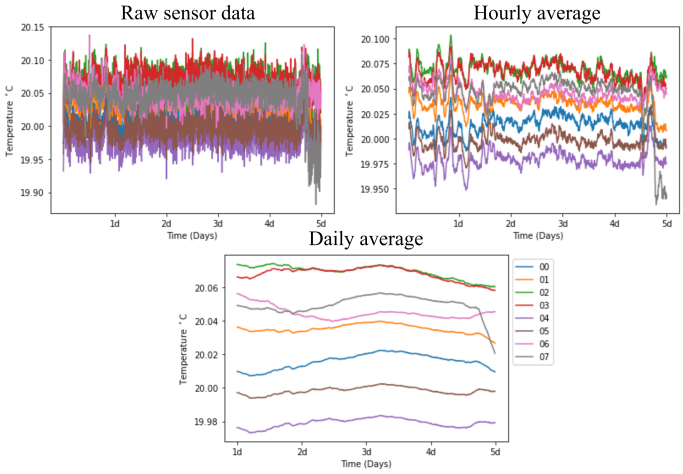

Fig. 2: The raw temperature readings from the eight sensors along with the hourly and daily rolling averages.

2.2. *Ordinary Kriging*

Kriging [5] is an interpolation method based on Gaussian processess with origins in geostatistics that, given a finite number of samples, provides predictions for the value of a function at unsampled locations under appropriate assumptions about the mean and covariance of the underlying process. Different variations of kriging are possible with respect to the chosen constraints on the mean and covariance. While Gaussian process regression assumes a known underlying mean function, we assume that the random process governing the temperature for our use case has a homogeneous unknown mean and use ordinary kriging to determine the temperature at the unsampled points in the volume.

Given N observed values (for eg. sensor readings) $\{T(\mathbf{x}_1), T(\mathbf{x}_2), \ldots, T(\mathbf{x}_N)\}$ at known locations $\{\mathbf{x}_1, \mathbf{x}_2, \ldots, \mathbf{x}_N\}$, the prediction $\hat{T}(\mathbf{x}_0)$ at a point $\mathbf{x}_0$ obtained via ordinary kriging is given by

$$\hat{T}(\mathbf{x}_0) = \sum_{n=1}^{N} w_n T(\mathbf{x}_n) = \mathbf{w}^T \mathbf{T}\,, \tag{1}$$

$$\text{with} \quad \mathbf{w}^T \mathbf{1} = \sum w_n = 1 \tag{2}$$

so as to ensure unbiasedness, i.e. $E[\hat{T}(\mathbf{x}_0)] = E[\hat{T}(\mathbf{x}_i)]$. The kriging estimate is determined by minimizing the kriging variance or the variance of the error-function $\epsilon(\mathbf{x}_0) = T(\mathbf{x}_0) - \hat{T}(\mathbf{x}_0)$,

$$\sigma_\epsilon^2 := \mathrm{Var}(\epsilon(\mathbf{x}_0)) = \mathrm{Var}(T(\mathbf{x}_0)) + \mathbf{w}^T C \mathbf{w} - 2\mathbf{w}^T D\,, \tag{3}$$

where $T(\mathbf{x}_0)$ is the true value at $\mathbf{x}_0$, C is the covariance matrix corresponding to the known samples and D is a vector whose components are the covariances between the observed values and the function value to be estimated at $\mathbf{x}_0$.

An appropriate prior covariance function $\mathrm{Cov}(\mathbf{x}_i, \mathbf{x}_j)$ is selected in order to determine $C_{ij} = \mathrm{Cov}(\mathbf{x}_i, \mathbf{x}_j)$ and $D_i = \mathrm{Cov}(\mathbf{x}_i, \mathbf{x}_0)$. Typically, the underlying process is assumed to be wide-sense stationary, i. e. $\mathrm{Cov}(\mathbf{x}_i, \mathbf{x}_j) = \mathrm{Cov}(|\mathbf{x}_i - \mathbf{x}_j|)$, and that the mean of the underlying process is constant. In order to ensure a smooth interpolation, the covariance function is generally chosen such that nearby points have a stronger correlation. The covariance is estimated using the variogram γ, which is related to the spatial covariance by

$$\gamma(h) = \mathrm{Var}(T(\mathbf{x}+\mathbf{h}) - T(\mathbf{x})) = \mathrm{Cov}(0) - \mathrm{Cov}(h) \tag{4}$$

and corresponds to the variance of the difference between values separated by a distance h. The variogram is approximated from the sampled values by fitting a chosen parametric function function to the empirical variogram

$$\gamma(h) = \frac{1}{2|N(h)|} \sum_{(i,j)\in N(h)} \left(T(\mathbf{x}_i) - T(\mathbf{x}_j)\right)^2\,, \tag{5}$$

where $N(h)$ denotes the set of all samples located at a distance $h = |\mathbf{h}|$ away from each other within a given tolerance. Common choices for the variogram function are linear, Gaussian and spherical.

2.3. *Motivation*

The characteristics of the sensors used in measurement rooms are dictated by factors such as operating cost, availability, interchangeability and ease of calibration. Often, sensors with different uncertainty characteristics need to be used in tandem. As the empirical variogram is computed solely from the sensor readings, the measurement uncertainty determined from its calibration is not directly taken into account in Kriging. The sensor measurement uncertainty can, in principle, be incorporated in the variogram (4) via the nugget effect, i.e. a discontinuity in γ at $h = 0$. For a Gaussian variogram model this results in

$$\gamma(h) = \begin{cases} 0 & \text{for } h = 0 \\ c_0 + c(1 - \exp(-3h^2/R^2)) & \text{for } h > 0 \end{cases}\,, \tag{6}$$

where the parameters c_0, c and R are determined by fitting the above function to the empirical variogram (5) such that c_0, the so-called *nugget* of the variogram, represents the variations at small distances and the sill $c + c_0$ corresponds to those at large distances. This way, the nugget effect is reflected in the kriging variance (3). However, the above formulation cannot account for the case where the sensors at the sampled locations have different associated uncertainties, i.e. for the heteroscedastic case. Heuristic methods to incorporate the individual sensor uncertainties in the nugget effect have been implemented [7, 8]. It is unclear, however, if these methods conform with the standards put forward in the Guide to the estimation of Uncertainty in Measurement (GUM, [9]) or if the computed kriging variances are a complete measure of uncertainty. Complementing the kriging variance with the propagated uncertainty of the sensor readings to the interpolated points is necessary for a more complete reliability statement.

3. IMPLEMENTATION DETAILS

The generation of the variogram and the estimation of the kriged values were implemented using the PyKrige [10] library. In particular the `OrdinaryKriging3D` class is used to fit a Gaussian variogram to the empirical variogram computed from the eight sensor outputs. The kriged values and the resulting variances were estimated on a grid of size 12×12×12 defined in the volume illustrated in Fig 1. The spatial interpolation achieved using Kriging is demonstrated in particular for the 200th measurement; see Table 1.

Table 1: Chosen Sensor Readings; cf. Fig. 1 for sensor labels.

Sensor	00	01	02	03
Reading (K)	20.01	20.04	20.08	20.07
Sensor	04	05	06	07
Reading (K)	19.98	19.99	20.06	20.05

3.1. Monte Carlo Uncertainty Estimation

The measurement uncertainties of the kriged estimates on the grid is obtained by propagating the sensor uncertainties using the Monte Carlo method in accordance with the first supplement of GUM [11]. In each trial, a random sample is drawn from the distribution modeling the uncertainty knowledge about the eight sensor readings. To do so, a multivariate normally distributed random variable with zero mean is used whose covariance is determined from the standard uncertainty of the individual sensors and is given by the 8×8 diagonal matrix

$$\mathrm{Cov}_{\mathrm{sensors}} = \mathrm{diag}\left(.025^2, 0.1^2, \ldots, 0.1^2\right) \qquad (7)$$

The sample drawn from the aforementioned distribution is added to the sensor readings given in Table 1. These values are then used in a single Monte Carlo trial to initialize an `OrdinaryKriging3D` object with the sensor positions as parameters and the interpolated temperatures are calculated on the 12×12×12 grid corresponding to the measuring region. These steps are repeated for $N_{\mathrm{trials}} = 10^6$ trials to estimate the mean and variance of the temperature at each point in the grid over all trials. A pseudocode for the Monte Carlo trials is provided in Algorithm 1.

4. RESULTS

The interpolated temperature is illustrated in Fig. 3 for two boundaries (W1 & W2) and the floor such that lighter colors correspond to higher temperatures. Kriging with a Gaussian variogram results in a smooth interpolation and the kriged temperature at a given point on the grid depends most strongly on the reading of the nearest sensor. The kriging variance determined for the sensor readings in Table 1 is illustrated along with the propagated measurement uncertainty determined using the Monte Carlo method in Fig. 4. The Monte Carlo simulation reproduces the sensor

Algorithm 1: Monte Carlo trials to propagate the sensor uncertainty to the volume grid

$T_{\mathrm{mean}} \leftarrow$ Zeros(12, 12, 12);
$\mathrm{var}_{\mathrm{temp}} \leftarrow$ Zeros(12, 12, 12);
for $i \leftarrow 1$ **to** N_{trials} **do**
  $[\widetilde{T}_1, \ldots \widetilde{T}_8] \leftarrow [T_1, \ldots T_8] + \mathcal{N}(0, \mathrm{Cov}_{\mathrm{sensors}})$;
  OK3D $\leftarrow$ OrdinaryKriging3D($[\mathbf{x}_1, \ldots \mathbf{x}_8]$, $[\widetilde{T}_1, \ldots \widetilde{T}_8]$);
  $T_{\mathrm{krig}} \leftarrow$ OK3D(X_{grid}, Y_{grid}, Z_{grid});
  $T_{\mathrm{mean}} \leftarrow T_{\mathrm{mean}} + T_{\mathrm{krig}}$;
  $\mathrm{var}_{\mathrm{temp}} \leftarrow \mathrm{var}_{\mathrm{temp}} + T^2_{\mathrm{krig}}$;
end
$\mathrm{var}_{\mathrm{temp}} \leftarrow \left(\mathrm{var}_{\mathrm{temp}} - T^2_{\mathrm{mean}}\right)/(N_{\mathrm{trials}} - 1)$;
$T_{\mathrm{mean}} \leftarrow T_{\mathrm{mean}}/N_{\mathrm{trials}}$;

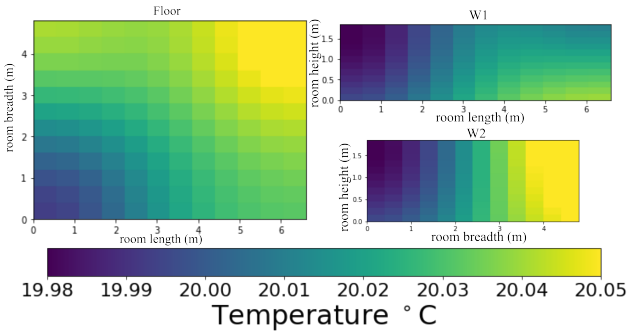

Fig. 3: The kriged temperatures along the floor (left) and the region boundaries, W1 & W2. The labels are as indicated in Fig. 1.

uncertainty at their respective physical locations and, like the interpolated temperature, the propagated uncertainty at a given point depends strongly on that of the nearest sensor. For instance, the propagated uncertainty is lower in the vicinity of sensor 00. The estimated uncertainty at unsampled locations is lower than the uncertainty at locations sampled by the sensors [12]. In contrast, the kriging standard deviation increases further away from the sensors and reflects the reliability of the interpolation.

4.1. Kriging as a data quality metric

In addition to spatial interpolation, kriging can potentially be used to assess the behavior of the sensors or to monitor the climate-controlled room for anomalous behavior. For instance, the temperature at the position of a given sensor can be compared to the estimate obtained at the same location by kriging the readings remaining sensors (eg., the temperature at $\mathbf{x}_0 = \mathbf{x}_1$ kriged using the readings at $\mathbf{x}_i$, $i = 2 \ldots 8$). The deviation of the sensor's readings from the kriged estimate can then be used as an assessment of its behavior based on a consensus of the remaining sensors can be made. The deviation of the individual sensor readings from the kriged estimate of the temperature at their

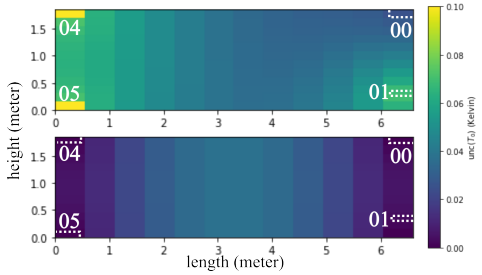

Fig. 4: Top: The Monte Carlo propagated measurement uncertainty along one boundary of the region. Bottom: The ordinary kriging variance calculated for the same boundary. The sensor numbers are as indicated in Fig. 1

position is illustrated in Fig. 5 for the entire duration of the experiment. The deviation in the kriged values at the posi-

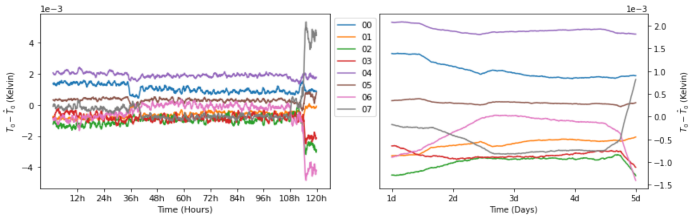

Fig. 5: The deviation of individual sensor readings from the value at the sensor position kriged from the remaining sensors. Left: hourly average, right: daily average.

tions of sensors 06 and 07 from their readings is noticeable in both the hourly and daily averages. While the raw sensor readings in Fig. 2 show a sharp change only in sensor 07, the deviation in the kriged estimate is also noticeable in its physical neighbor, i.e., sensor 06. A smaller deviation is also evident for sensors 03 and 06. In this way, it is possible to rule out a sensor failure in favour of a localized temperature change brought about, for instance, by the opening of the nearby door. Conversely, a deviation in the reading of an individual sensor could be indicative of a malfunction.

5. CONCLUSIONS

A method for interpolating room temperatures and computing the associated measurement uncertainty from a limited number of sensor readings using ordinary kriging was presented. The measurement uncertainty propagated from the sensors to a point in a subvolume of the room differs significantly from the interpolation standard deviation in the same region determined from kriging the sensor readings. The interpolated temperatures and the corresponding uncertainties depend most strongly on those of the nearest sensor such that the propagated uncertainty is smaller in the vicinity of the sensor with lower uncertainty. A potential application of kriging for a consensus based quality-of-sensing assessment was also presented. By comparing a given sensor reading with the kriged value at its position determined from the remaining anomalous sensor readings can be identified. In future research, the effect of adding and removing sensors to the setup as well as a comparitive study with conventional Gaussian process regression will be carried out.

ACKNOWLEDGEMENTS

Research for this paper was co-financed within the project GEMIMEG-II of the Federal Ministry for Economic Affairs and Climate Action (BMWK) [grant reference GEMIMEG 01 MT20001E]. We also thank Gerd Bauer, Markus Nagler and Daniel Heißelmann for their valuable insights and comments.

REFERENCES

[1] Platform Industrie 4.0 and Federal Ministry of Education and Research, “Zukunftsbild Industrie 4.0,” 2013.

[2] B. Khaleghi, A. Khamis, F. Karray and S. Razavi, “Multisensor data fusion: A review of the state-of-the-art”, *Information Fusion*, vol. 14, pp. 28–44, 2013.

[3] VDI/VDE Technical Specification 2627, “Measuring rooms - Classification and characteristics - Planning and execution”, 2015.

[4] R. Jedermann, J. Palafox-Albarrán, P. Barreiro, L. Ruiz-García, J. Ignacio Robla and W. Lang, “Interpolation of spatial temperature profiles by sensor networks”, SENSORS, 2011 IEEE, pp. 778–781, 2011.

[5] P. Diggle, J. Tawn and R. Moyeed, “Model-based geostatistics”, *Journal Of The Royal Statistical Society: Series C (Applied Statistics)*. vol. 47, pp. 299–350, 2013.

[6] G. Matheron, *The Theory of Regionalized Variables and Its Applications*, Les Cahiers du Centre de Morphologie Mathematique in Fontainebleu, Paris, 1971.

[7] F. Cecinati, A. Moreno-Ródenas, M. Rico-Ramirez, M. Ten Veldhuis and J. Langeveld, “Considering Rain Gauge Uncertainty Using Kriging for Uncertain Data”, *Atmosphere*, vol. 9, no. 11, 2018.

[8] C. Mazzetti and E. Todini, Combining Weather Radar and Raingauge Data for Hydrologic Applications, in: P. Samuels, S. Huntington, W. Allsop, J. Harrop (Eds.), Flood Risk Management: Research and Practice, Taylor & Francis Group: London, UK, 2009, ISBN 9780415485074.

[9] Joint Committee for Guides in Metrology, JCGM 104:2009 An introduction to GUM and related documents, available at: `https://www.bipm.org/documents/20126/2071204/JCGM_104_2009.pdf` (accessed 10 June 2022).

[10] B. Murphy, S. Müller and R. Yurchak, PyKrige: v1.6.1, 2020, DOI: 10.5281/zenodo.3738604.

[11] Joint Committee for Guides in Metrology, JCGM 101:2008 Supplement 1: Propagation of distributions using a Monte Carlo method, available at: `https://www.bipm.org/documents/20126/2071204/JCGM_101_2008_E.pdf` (accessed 11 April 2022).

[12] D. R. White, “Propagation of Uncertainty and Comparison of Interpolation Schemes”, *International Journal of Thermophysics*, vol. 38, no. 39, 2017.